

# Cold Discharge of CF<sub>3</sub>I in a Simulated Aircraft Engine Nacelle<sup>1</sup>

JIANN C. YANG<sup>2</sup>, SAMUEL L. MANZELLO, and MARC R. NYDEN

Building and Fire Research Laboratory

National Institute of Standards and Technology

100 Bureau Drive, Gaithersburg, Maryland 20899, USA

MICHAEL D. CONNAGHAN

U.S. Army CECOM Research, Development, and Engineering Center

Fort Belvoir, Virginia 22060, USA

## ABSTRACT

An aircraft engine nacelle simulator was built to study the dispersion behavior of CF<sub>3</sub>I, a potential Halon 1301 (CF<sub>3</sub>Br) replacement, at temperatures below -22 °C (normal boiling point of CF<sub>3</sub>I). The experimental fixture consists of a simulated engine nacelle with baffles, an agent release port, observation windows, and two measurement locations. The simulator has a configuration and dimensions commensurate with a typical small engine nacelle. The entire facility was placed inside a large environmental test chamber. Agent discharge experiments were conducted at -40 °C. The dispersion of CF<sub>3</sub>I was assessed by measuring the concentration at the two measurement locations in the simulator using fiber-optic-based UV spectrometers. Baseline agent dispersion performance was also established at room temperature. Compared to the measurements obtained at room temperature, there was a significant reduction in the peak agent concentration in the cold temperature release, and a fire suppression system designed based on room-temperature test data may fail to provide adequate fire protection at -40 °C.

**KEYWORDS:** Halon replacement, engine nacelles, UV spectrometers, fire suppression

## INTRODUCTION

An aircraft engine nacelle refers to the region between the engine body and its casing. Fuel and hydraulic lines, pumps, and lubrication systems are located within the nacelle. Air is vented through the nacelle to prevent any build-up of combustible vapors, and underside drain holes are used to mitigate potential pooling of flammable fluids as a result of a leak. Depending on the configuration of the aircraft, the fire suppression bottle is mounted either adjacent to the engine nacelle or at a location several meters away from the nacelle, where upon release the agent is transported through piping to the fire zone.

---

<sup>1</sup> Official contribution of the National Institute of Standards and Technology not subject to copyright in the United States.

<sup>2</sup> Corresponding author. Tel: 301-975-6662; fax: 301-975-4052; e-mail: jiann.yang@nist.gov

Most aircraft fire suppression bottles for engine nacelle fire protection are normally filled with liquid  $\text{CF}_3\text{Br}$  (Halon 1301) to about half of the bottle volume, and the bottle is then pressurized with nitrogen to a specified equilibrium pressure (typically 4.1 MPa) at room temperature. The purpose of using the pressurization gas is to expedite the discharge of the agent and to facilitate the dispersion of the agent. Without nitrogen pressurization, the bottle pressure, which is simply the vapor pressure of the agent, can be so low, especially at cold ambience, that there is not enough driving force to rapidly expel the agent from the bottle in case of a fire.

Present military specification (MIL-E-22285) [1] for  $\text{CF}_3\text{Br}$  in engine nacelle applications call for a discharge time of less than 0.5 s and an amount of agent corresponding to a dwell time of 0.5 s throughout the protected nacelle space with an agent volume fraction of at least 0.06 at normal cruising condition. The certification process for the fire suppression system requires the use of a Halonyzer, a Federal Aviation Administration certified instrument, with 12 measurement probes positioned throughout the protected space to monitor the temporal  $\text{CF}_3\text{Br}$  concentration upon the discharge of the agent.

Due to its adverse effect on the ozone layer, Halon 1301 has been banned from production in the United States since 1994 in compliance with the Montréal Protocol On Substances That Deplete The Ozone Layer. Many studies have since been conducted to identify alternatives to replace Halon 1301. Trifluoroiodomethane ( $\text{CF}_3\text{I}$ ) has been proposed as a potential replacement for Halon 1301 in aircraft engine nacelle and dry bay fire protection applications [2,3]. Dry bays are closed spaces adjacent to the fuel tank or hydraulic lines in the fuselage and wings and are normally cluttered with avionics. Before  $\text{CF}_3\text{I}$  can be considered as a potential drop-in replacement agent for such applications, several operational and technical issues need to be addressed or examined. The focus of this study is on aircraft engine nacelle applications.

One important aspect pertinent to  $\text{CF}_3\text{I}$  applications in engine nacelle is the discharge behavior of the agent when it is exposed to ambient temperatures well below its normal boiling point. The cold temperature release finds its applications in the cold start of an engine in a cold environment or in high-altitude cruising conditions.

Table 1 lists some of the physical properties of  $\text{CF}_3\text{I}$  and  $\text{CF}_3\text{Br}$ . Since  $\text{CF}_3\text{I}$  has a normal boiling point of  $-22\text{ }^\circ\text{C}$ , the dispersion of  $\text{CF}_3\text{I}$  into air at temperatures down to  $-40\text{ }^\circ\text{C}$  may not be as effective as Halon 1301, which has a normal boiling point of  $-57.8\text{ }^\circ\text{C}$ .

Although the release of  $\text{CF}_3\text{I}$  (at room temperature or chilled to about  $-40\text{ }^\circ\text{C}$ ) into a fire compartment and an engine nacelle simulator at ambient room temperature has been examined [4,5], the discharge of cold  $\text{CF}_3\text{I}$  into a cold ambience has not been performed, or at least has not been documented in open literature. To the best of our knowledge, there is only one corporate internal report [6], which describes a study of the release of cold  $\text{CF}_3\text{I}$  into a well-mixed cold *enclosure* with no airflow. Careful examination of the data indicated some deterioration in the distribution of  $\text{CF}_3\text{I}$  within the enclosure when compared to room temperature conditions. To assure that there is no substantial deterioration in dispersion performance of  $\text{CF}_3\text{I}$  under cold temperature applications, discharge tests in an aircraft engine nacelle at temperatures below  $-22\text{ }^\circ\text{C}$  are needed. The temperature of  $-40\text{ }^\circ\text{C}$  was selected in this study because it was below the normal

boiling point of  $\text{CF}_3\text{I}$  and was the lowest operating temperature for some of the equipment used in the experiments. Note that in some cases, military specifications require an operating temperature of  $-54\text{ }^\circ\text{C}$  ( $-65\text{ }^\circ\text{F}$ ).

Table 1. Selected physical properties of  $\text{CF}_3\text{I}$  and  $\text{CF}_3\text{Br}$  [4].

Agent	Molecular weight (kg/mol)	$T_b$ ( $^\circ\text{C}$ )	$T_c$ ( $^\circ\text{C}$ )	$P_c$ (MPa)	$\rho_c$ ( $\text{kg}/\text{m}^3$ )	$\Delta H_v$ (kJ/kg)
$\text{CF}_3\text{I}$	0.196	-22.0	122.0	4.04	871	106
$\text{CF}_3\text{Br}$	0.149	-57.8	67.0	4.02	745	111

$T_b$  is the normal boiling point;  $T_c$  is the critical temperature;  $P_c$  is the critical pressure;  $\rho_c$  is the critical density;  $\Delta H_v$  is the latent heat of vaporization at  $T_b$ .

## APPARATUS

The experimental apparatus consisted of a simulated engine nacelle with baffles, an agent release port, four observation windows, and two measurement ports. Figure 1 is a schematic of the simulator. The annulus of the simulator had an inside diameter of 0.6 m and an outside diameter of 0.9 m, resulting in a cross-sectional area of  $0.35\text{ m}^2$ . The length (2 m) of the simulator was comparable to the distance between the agent injection port and the downstream end of a typical small engine nacelle. The baffle height was 0.075 m. The baffles were used to mimic a complicated flow path for the agent as in the case of a real nacelle. Two longitudinal ribs with the same height as the baffles were placed on the outer surface of the inner core of the nacelle between the inner forward and aft baffles, see Fig. 1. The ribs were used as barriers to the agent flowing circumferentially. The simulator was fabricated of 3.2 mm thick stainless-steel sheet metal.

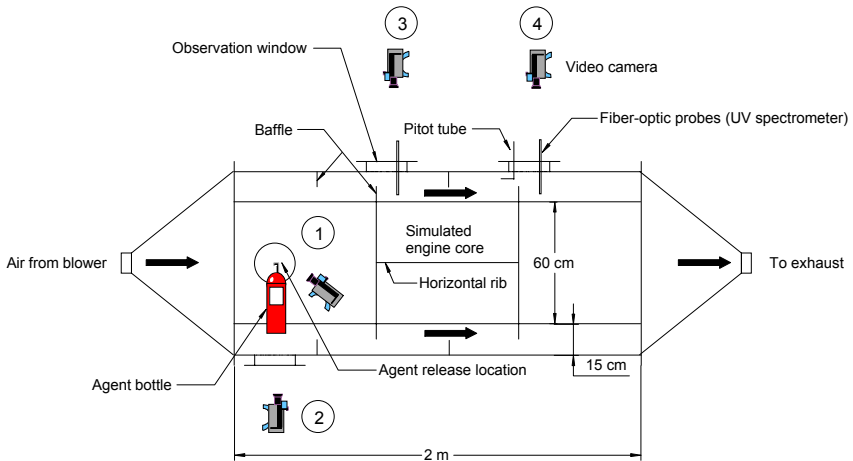


Fig. 1. Schematic of the test fixture.

A receiver bottle (Pacific Scientific<sup>3</sup>, P/N 36200122) with an internal volume of 2.36 L was used to store CF<sub>3</sub>I for discharge. A fast-response static pressure transducer (uncertainty  $\pm 10$  kPa specified by the manufacturer) was mounted on the receiver bottle to monitor the pressure inside the bottle during filling and discharge. A K-type thermocouple (uncertainty  $\pm 1$  °C) was inserted into the bottle to record the temperature of the liquid agent before discharge. A quick-acting solenoid valve (Pacific Scientific, P/N 36400036) was used to release the agent. To tailor the agent discharge time ( $\approx 0.5$  s), a reducer was placed at the valve exit. The agent was released through a vertical tee at the end of a short stainless-steel tubing (i.d. = 15.9 mm, o.d. = 19.1 mm) connected to the reducer. Four CCD cameras (30 frames/s) were used to observe the agent discharge behavior at the release port (Camera 1), at a location in the bottom of the simulator to observe any pooling of agent (Camera 2), and at the two concentration measurement locations (Cameras 3 and 4), respectively. A frequency-controlled, variable-speed blower provided airflow through the nacelle simulator. The maximum air speed at room temperature in the annulus, measured using a pitot tube, can reach 9.2 m/s.

To achieve an operating temperature of  $-40$  °C, the entire facility was placed inside the U.S. Army environmental test chamber at Ft. Belvoir, and the cold discharge experiments were conducted inside the chamber. The chamber has an interior dimension of 2.74 m (H)  $\times$  3.35 m (W)  $\times$  3.66 m (L) and a 1.83 m  $\times$  1.83 m sliding door. The lowest temperature attainable in the environmental test chamber is  $-54$  °C. Discharge experiments in room temperature were also conducted inside the chamber with the refrigeration unit turned off to establish baselines for comparisons.

The experimental procedure involved the following steps. The receiver bottle was first immersed in dry ice and connected to the CF<sub>3</sub>I supply bottle, which was placed on an electronic balance (uncertainty of  $\pm 1$  g) to monitor the amount of agent transferred to the receiver bottle. The dry ice was used to condense the CF<sub>3</sub>I vapor in the receiver bottle. The supply bottle was slightly warmed using two 120 V floodlights to increase the vapor pressure to facilitate the transfer of CF<sub>3</sub>I vapor to the receiver bottle. When the amount of agent in the receiver bottle reached the target mass, the bottle was then removed from the dry ice, warmed back to room temperature, and weighed on the electronic balance to determine the actual mass in the bottle. The receiver bottle was then pressurized with nitrogen to 4.12 MPa. Shaking the bottle intermittently and vigorously was required before the final equilibrium pressure was attained. The amount of nitrogen added was obtained by weighing the filled bottle. The bottle was now ready for the discharge experiments. For cold temperature conditions, the environmental test chamber and the receiver bottle were cooled down to approximately  $-40$  °C before a test was commenced. Two contact K-type thermocouples were attached on the front and aft of the simulator external skin to monitor the ambient temperature of the chamber. In addition, a bare-beaded K-type thermocouple was placed in the annulus to measure the airflow temperature through the nacelle.

---

<sup>3</sup> Certain commercial products are identified in this paper in order to specify adequately the equipment used. Such identification does not imply recommendation by the National Institute of Standards and Technology, nor does it imply the equipment is the best available for the purpose.

Given the simulated nacelle volume and airflow, the amount of agent required for a fixed injection period ( $< 0.5$  s for typical nacelle applications) was estimated using the generic nacelle modeling results discussed in Hamins *et al.* [7]. The agent bottle was charged with  $\approx 1$  kg of  $\text{CF}_3\text{I}$  and then pressurized with nitrogen to the desired pressure (4.21 MPa) at room temperature. Table 2 lists the experimental matrix. The airflow through the simulator was maintained at  $1.5 \text{ kg/s} \pm 0.1 \text{ kg/s}$  (mean  $\pm$  standard deviation).

Table 2. Experimental matrix.

Nominal initial conditions of vessel	Nominal conditions of vessel before discharge	Nominal conditions in the simulator
22 °C and 4.12 MPa	-40 °C at prevailing $P$	-40 °C
22 °C and 4.12 MPa	22 °C and 4.12 MPa	22 °C (baseline)
22 °C and 4.12 MPa	22 °C and 4.12 MPa	-40 °C

The dispersion effectiveness of  $\text{CF}_3\text{I}$  was assessed based upon concentration measurements at the two locations inside the engine nacelle simulator (see Fig. 1). The number of measurement locations was limited *solely* by the cost of the instruments. Note that the intent of this work is not to address the certification process, which requires twelve measurement locations. The measurements were made using two Ocean Optics S2000 UV/VIS fiber-optic spectrometers. The optical components consisted of deuterium/tungsten source, four (UV grade quartz) collimating lenses, and 300  $\mu\text{m}$  diameter optical fibers. These were arranged to provide two measurement locations (coincident with Cameras 3 and 4) approximately 0.75 m apart along the direction of the airflow in the engine nacelle testing apparatus. A bifurcated fiber (1 m in length, coupled with a 5 m extension) was used to connect the source to a pair of collimating lenses secured by brackets to the Plexiglas® viewing windows located on the top of the apparatus. The source radiation emanating from each lens was transmitted over a 0.038 m optical path (perpendicular to the airflow) to an opposing set of collimating lenses connected by independent optical fibers (5 m in length) to the master and slave spectrometers. Although the manual indicated that these optical components should have a spectral range from 200 nm to 850 nm, we found that very little throughput at wavelengths shorter than 250 nm.

The spectrometer settings used for the measurements in the nacelle testing apparatus were as follows. The spectrometers were software triggered by an electronic timer. The integration time (analogous to the shutter speed) was set at 30 ms, and the pixel resolution of the analogue to digital converter (ADC) was set at 10, which amounts to a spectral resolution of only about 3 nm. With this configuration, we were able to achieve a data acquisition rate of approximately 12 single scan spectra (6 at each location) per second to capture the time dependent details of the agent discharge. An estimate of the uncertainty (one standard deviation) of our measurements was obtained by comparing results at these settings to more accurate values obtained after signal averaging 100 scans at the full resolution of the spectrometer ( $\approx 0.3$  nm). Based on this analysis, the  $\text{CF}_3\text{I}$  partial pressures reported in this paper are accurate to  $\pm 15\%$ .

The UV spectrometer was calibrated at 295 K using a quartz cell with an optical path length of 0.075 m. The cell was first evacuated to 1.33 Pa. Then, a fixed amount of  $\text{CF}_3\text{I}$

vapor was metered into the cell by monitoring the cell pressure. Spectra were taken using an integration time of 30 ms and a pixel resolution of 10. Figure 2 shows a typical CF<sub>3</sub>I absorption spectrum. Note that the peak absorbance for CF<sub>3</sub>I centers around 270 nm. The calibration curve (at  $\lambda = 300$  nm and 295 K), which is a plot of absorbance ( $A$ ) against concentration ( $C$ , molecules cm<sup>-3</sup>), is shown in Fig. 3.

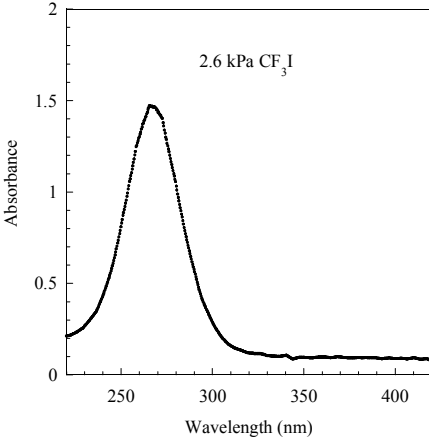


Fig. 2. An absorption spectrum of CF<sub>3</sub>I.

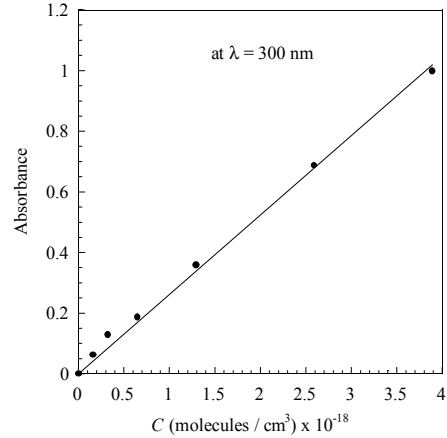


Fig. 3. Calibration curve at 300 nm.

The Bouguer-Beer-Lambert law is expressed as

$$A(\lambda) = -\log\left[\frac{I(\lambda)}{I_o(\lambda)}\right] = \frac{C\sigma(\lambda,T)L}{2.303} \quad (1)$$

where  $I(\lambda)$  and  $I_o(\lambda)$  are the incident and transmitted intensities through the cell respectively,  $\sigma(\lambda,T)$  is the absorption cross section (cm<sup>2</sup>),  $L$  is the optical path length (cm),  $T$  is the temperature, and  $\lambda$  is the wavelength. Note that the absorption cross-section is a function of wavelength and temperature. Using the ideal gas law, Eq. 2 gives the relationship between  $C$  and the partial pressure  $p$  (Pa) at 295 K.

$$C = 2.44 \times 10^{14} p \quad (2)$$

From Eq. 1, the absorption cross section can be obtained from the slope of the calibration curve. A linear regression line is fitted through the data points in Fig. 3, and the absorption cross-section of CF<sub>3</sub>I is  $8.1 \times 10^{-20}$  cm<sup>2</sup>, which is comparable to the value of  $8.9 \times 10^{-20}$  cm<sup>2</sup> at  $\lambda = 300$  nm and 295 K to 300 K in the literature [8]. Since the calibration was performed at 295 K, a correction for the temperature effect on the absorption cross section is necessary to obtain the CF<sub>3</sub>I partial pressure at other prevailing temperature, using the following equation [8]:

$$\sigma(\lambda, T) = \sigma(\lambda, 298 \text{ K}) \exp[B(\lambda)(T - 298)] \quad 210 \text{ K} < T < 300 \text{ K} \quad (3)$$

The concentration  $C$  of  $\text{CF}_3\text{I}$  at any temperature was calculated from the absorbance measurement using Eqs. 1 and 3. At 300 nm,  $B = 4.876 \times 10^{-3} \text{ K}^{-1}$  [8]. The partial pressure of  $\text{CF}_3\text{I}$  was then obtained using the ideal gas law at the *prevailing* temperature. However, the temperature effect on the absorption cross section was found to be negligible in the concentration calculations.

An electronic timer was used to coordinate the experimental sequence of events. At  $t = 0$  s, a signal was sent from the timer to trigger the data acquisition system to record the pressure of the discharge bottle and the pitot tube output at a sampling rate of 200 Hz. At  $t = 1$  s, the timer initiated the two UV spectrometers, and at  $t = 2$  s, the solenoid valve was activated to discharge the  $\text{CF}_3\text{I}$ /nitrogen mixture from the bottle into the engine nacelle simulator.

## RESULTS AND DISCUSSION

Figure 4 shows the temporal variation of pressure inside the bottle during a typical discharge. The initial time ( $t = 0$ ) corresponds to the time when the solenoid valve was opened. In the figure, the prevailing bottle pressure before discharge at  $\approx -40^\circ\text{C}$  is much lower than that at room temperature. Due to the reduction in the initial bottle pressure, the discharge time ( $\approx 0.24$  s) of the cold *liquid* agent is much longer than that ( $\approx 0.16$  s) of the baseline case; the liquid discharge time corresponds to the transition point in the pressure vs. time curve [9]. The observations from Camera 1 also showed that the agent discharge time at  $\approx -40^\circ\text{C}$  was longer than that at room temperature.

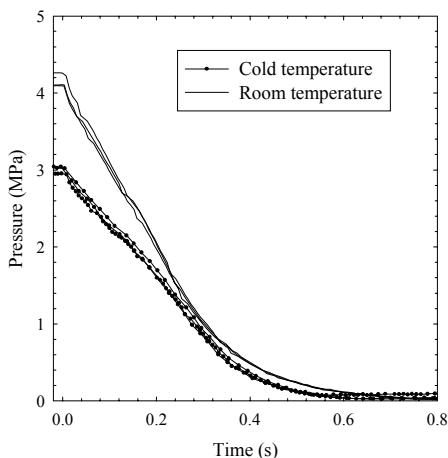


Fig. 4. Variation of bottle pressure during discharge at room and cold temperatures.

When  $\text{CF}_3\text{I}$  was discharged at room temperature, the observations obtained from Camera 2 showed that a small amount of  $\text{CF}_3\text{I}$  pooled in the bottom of the simulator upon release. However, the liquid  $\text{CF}_3\text{I}$  boiled off within 66 ms. When  $\text{CF}_3\text{I}$  was discharged at  $-40^\circ\text{C}$ , a significant amount of liquid  $\text{CF}_3\text{I}$  pooled at the bottom of the nacelle upon release. The liquid  $\text{CF}_3\text{I}$  evaporated slowly and remained for many seconds ( $> 60$  s) before complete evaporation. The observations from Cameras 3 and 4 showed that a cloud of  $\text{CF}_3\text{I}$  passed

through the field of view of the cameras after agent discharge. The observations from Cameras 3 and 4 were qualitatively similar for the discharge of  $\text{CF}_3\text{I}$  at room temperature and  $-40\text{ }^\circ\text{C}$ .

The difference in pooling tendency described above can be explained as follows. Consider a 2.36 L container with 1 kg of  $\text{CF}_3\text{I}$  pressurized with nitrogen to 4.12 MPa at  $22\text{ }^\circ\text{C}$ . If the container is cooled down to  $-40\text{ }^\circ\text{C}$  before release, the final pressure of the container is estimated to be 2.8 MPa using the computer code (PROFISSY) developed by the National Institute of Standards and Technology [4,10]. The code is based on the calculations of vapor-liquid phase equilibria using the extended corresponding-states principle. Assuming the discharge of the liquid agent from the container is an isentropic process from the initial container pressure to atmospheric pressure, the final states of the agent can be calculated using the computer code (FISSYCS), which is a modified version of PROFISSY [4]. Table 3 tabulates the calculated results for the two conditions. The liquid mole fraction (the percent of agent/nitrogen mixture still remained in liquid phase after the isentropic expansion process) is substantially higher at  $-40\text{ }^\circ\text{C}$  than at  $22\text{ }^\circ\text{C}$ . Such a high liquid fraction should result in significant pooling upon agent release from the bottle. The combined effects of liquid pooling and slow evaporation at  $-40\text{ }^\circ\text{C}$  will have an adverse impact on the subsequent dispersion of the agent/nitrogen mixture in the nacelle.

Table 3. Liquid fraction of  $\text{CF}_3\text{I}/\text{N}_2$  mixture after isentropic expansion to 0.101 MPa.

Initial conditions	Liquid fraction (%)
$22\text{ }^\circ\text{C}$ at 4.12 MPa	70
$-40\text{ }^\circ\text{C}$ at 2.8 MPa	90

Although full  $\text{CF}_3\text{I}$  spectra were obtained in each test, a common practice used in spectroscopy to obtain the concentration measurements from the spectra is based on the wavelengths at the peak absorbance or its vicinity. The absorbance at 300 nm was used to obtain the  $\text{CF}_3\text{I}$  concentration because saturation of the detector at  $\approx 280\text{ nm}$  was observed under certain test conditions. The concentration of  $\text{CF}_3\text{I}$  thus obtained is shown for both the room and cold temperature releases in Figs. 5 and 6 for the two measurement locations, respectively. The initial time ( $t = 0$ ) in the figures corresponds to the initiation of the agent release. Although three runs were performed at each condition with similar observations, only a single run for each condition is shown in the figure for clarity. The arrival times of the agent at the two measurement locations were clearly captured in the figures. Some salient features are noted in the two figures.

For the room temperature release, an initial spike was observed at the forward measurement location. This was due to the presence of a two-phase (liquid droplet-laden) flow because the off-resonance spectral measurement at 500 nm also showed a peak at the same time. The two-phase flow was the result of break-up of the liquid core at the discharge port into droplets. The off-resonance extinction at 500 nm indicated that liquid  $\text{CF}_3\text{I}$  droplets were present for only a short period of time ( $< 2\text{ s}$ ) immediately following the discharge. Therefore, it can be argued that the concentration measurements after the initial spike in Fig. 5 was due largely to the  $\text{CF}_3\text{I}$  vapor with minimal or negligible contribution from the droplets. The off-resonance spectral measurement at

500 nm in the aft location indicated that no droplets were present. The absence of the droplets and the much lower  $\text{CF}_3\text{I}$  concentration (see Fig. 6) at this location indicated that the current nacelle simulator had indeed created a very challenging environment for agent dispersion, a condition which is generally true for a real engine nacelle. Furthermore, the generic nacelle model [7] provided a reasonable estimate of the amount of agent needed to achieve the required extinguishing concentration at two measurement locations in the current nacelle. Halon 1301 and  $\text{CF}_3\text{I}$  have similar heptane cup-burner extinguishing concentration, a volume fraction of 0.032 [2]. Assuming that the military specification for Halon 1301 can be applied to  $\text{CF}_3\text{I}$ , the measurements in Figs. 5 and 6 suggest that a volume fraction of 0.06 can be attained over a duration of 0.5 s in both locations at room temperature.

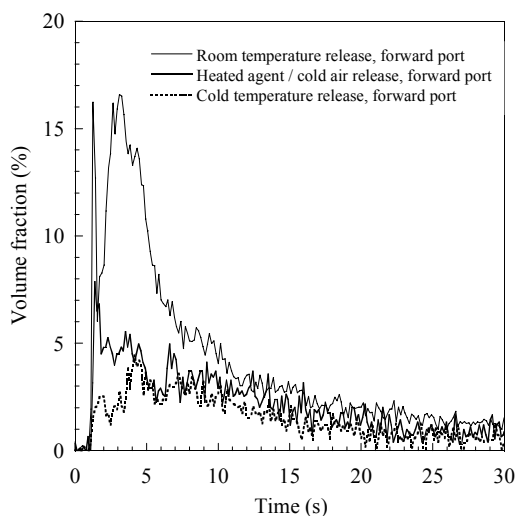


Fig. 5.  $\text{CF}_3\text{I}$  concentration profiles at the forward port.

For cold temperature release, the off-resonance spectral measurements at 500 nm did not indicate the initial presence of droplets at both forward and aft measurement locations. The absence of the droplets was due partly to the reduction in the initial bottle pressure ( $\approx 3 \text{ MPa}$  vs.  $\approx 4.1 \text{ MPa}$  at room temperature), which would impart less momentum to the droplets upon the release of the agent. Droplets with less momentum were less likely to be transported to the two measurement locations. The combined effect of low bottle pressure and large liquid fraction in cold temperature release (see discussion above) might generate larger droplets as a result of poor atomization of the liquid core, thus hindering the droplets to follow the airflow. Similar to the room temperature release, the concentration at the forward location was higher than that at the aft. However, the difference was not as significant as in the case of room temperature release. The most important finding from this study was that there was a significant reduction in the agent concentration in the cold temperature release. At the forward measurement location, a reduction of a factor of almost 3 was observed at the peak concentration. At both locations, the agent concentration measurements were always *below* a volume fraction of 0.06.

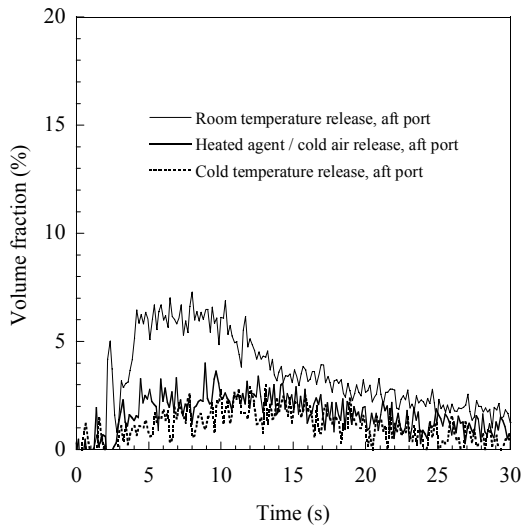


Fig. 6.  $\text{CF}_3\text{I}$  concentration profiles at the aft port.

One operational strategy to mitigate the poor dispersion of  $\text{CF}_3\text{I}$  for cold temperature applications has been proposed, namely, warming the bottle before being released into the cold ambience. Figures 5 and 6 illustrate, respectively, the concentration measurements at the two locations in the nacelle simulator when the agent was released at  $\approx 20^\circ\text{C}$  and the airflow through the nacelle was maintained at  $\approx -40^\circ\text{C}$ . The concentration levels obtained under this condition were still much lower than those at room temperature; however, some improvement was clearly noted when compared to the results at cold temperature.

To further illustrate this approach, we resorted to thermodynamic calculations using PROFISSY, FISSYCS, and the same initial bottle conditions at room temperature (1 kg of  $\text{CF}_3\text{I}$  in a 2.36 L bottle, pressurized with nitrogen to 4.12 MPa at  $22^\circ\text{C}$ , see discussion above). Note that in the following analysis, the heat transfer between the flashing spray and the nacelle surroundings was not considered. The calculations were performed as follows. First, a final state of the bottle was obtained using PROFISSY to simulate heating or cooling of the bottle. The state was then used as input for FISSYCS to obtain the amount of liquid fraction resulted from an isentropic process from the prevailing pressure to 0.101 MPa.

Figure 7 shows the calculated liquid fraction as a function of temperature. The liquid fraction decreases with increasing bottle temperature. However, there is a discontinuity at about  $94^\circ\text{C}$ . At temperatures below the discontinuity temperature, the initial state is liquid-phase, the isentropic process results in a liquid-vapor system. At temperatures above the discontinuity temperature, PROFISSY predicted a single-phase gaseous state before the isentropic process. The discontinuity is the result of the occurrence of a two-phase system due to the isentropic process. If the strategy is to decrease the liquid fraction, heating the bottle up to a temperature before the discontinuity temperature is reached seems to be an option. Although heating the bottle above the discontinuity temperature appears to be a better choice from the figure, a dichotomy exists. On the one

hand, the resulting liquid fraction is much lower than that at any temperature below the discontinuity temperature. On the other hand, the isentropic process inadvertently transforms a gaseous phase, which facilitates the dispersion of the agent, back to a liquid-vapor phase, which may hinder agent transport through cluttered space in the nacelle. However, system constraints (*e.g.*, bottle operating pressure and space) on a specific aircraft platform may ultimately limit the implementation of either approach because the bottle pressure is a function of temperature. Although the above argument provides some thermodynamic basis for examining the feasibility of heating the bottle to improve dispersion for cold temperature applications, the interaction of a flashing spray with cold nacelle surfaces may also play an important role in determining subsequent agent dispersion. Further experiments are needed to validate the concept.

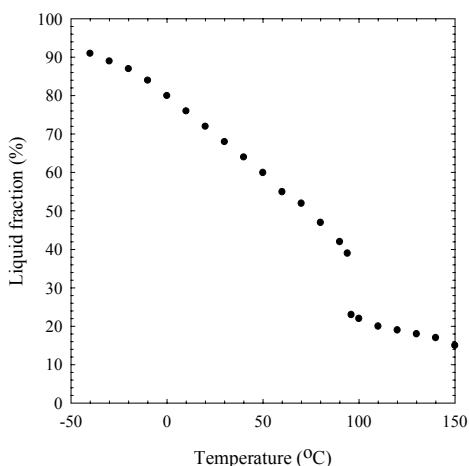


Fig. 7. Calculated liquid fraction as a function of bottle temperature.

## CONCLUSIONS

A series of discharge tests have been conducted at  $-40\text{ }^{\circ}\text{C}$  in an aircraft engine nacelle simulator placed inside an environmental test chamber. The results from the two measurement locations in the nacelle have shown that the dispersion of  $\text{CF}_3\text{I}$  under this condition with the equipment and the discharge nozzle used is not very effective and there is substantial deterioration in agent concentration. If the military specification for Halon 1301 extinguishing concentration can be applied to  $\text{CF}_3\text{I}$  (volume fraction of 0.06 for 0.5 s), the concentration levels at the two measurement locations in the nacelle never exceed the extinguishing concentration requirement. The situation worsens at the location further away from the agent injection port. If the agent extinguishing concentration for the engine nacelle is designed, based on room-temperature test data, our measurements indicate that serious consequences may result when the agent is used at a temperature lower than its normal boiling point.

## ACKNOWLEDGMENTS

This research is part of the Department of Defense's Next Generation Fire Suppression Technology Program (NGP), funded by the DoD Strategic Environmental Research and

Development Program (SERDP). Dr. Richard G. Gann of the National Institute of Standards and Technology (NIST) is the technical program manager. We would also like to thank Dr. Vladimir Orkin of the Chemical Sciences and Technology Laboratory (CSTL) of NIST for his assistance in the calibration of the UV spectrometer and Dr. William L. Grosshandler of our laboratory for many stimulating discussions and encouragement. SLM also acknowledges the financial support from the National Research Council Postdoctoral Research Associateship.

## REFERENCES

- [1] Military Specification, MIL-E-22285 (Wep), *Extinguishing System, Fire, Aircraft, High-Rate-Discharge Type, Installation and Test of*, 11 December 1959, Amendment – 1, 27 April 1960.
- [2] Grosshandler W.L., Gann R.G., Pitts W.M. (eds.), Evaluation of Alternative in-Flight Fire Suppressants for Full-Scale Testing in Simulated Aircraft Engine Nacelles and Dry Bays, NIST SP 861, April 1994, U.S. Department of Commerce, Washington, DC.
- [3] Gann R.G. (ed.), *Fire Suppression System Performance of Alternative Agents in Aircraft Engine and Dry Bay Laboratory Simulations*, Volumes I and II, NIST SP 890, U.S. Department of Commerce, Washington, DC, November 1995.
- [4] Yang, J.C., Cleary, T.G., Vázquez, I., Boyer, C.I., King, M.D., Breuel, B.D., Womeldorf, C.A., Grosshandler, W.L., Huber, M.L., Weber, L., and Gmurczyk, G., “Optimization of system discharge,” in Chapter 8, *Fire Suppression System Performance of Alternative Agents in Aircraft Engine and Dry Bay Laboratory Simulations*, Vol. I, Gann, R.G. (ed.), NIST SP 890, U.S. Department of Commerce, Washington, DC, November 1995.
- [5] Guesto-Barnak, D., Sears, R., Simpson, T., “Engine nacelle fire protection using non-ozone depleting fire suppressants,” *Proceedings of International Conference on Ozone Protection Technologies*, pp. 515-524, Washington, D.C., October 21-23, 1996.
- [6] Meserve, W.J., “Personal communication,” Pacific Scientific, HTL/KIN-Tech Division, Document Number 51750579, Duarte, California, May 2000.
- [7] Hamins, A., Cleary, T.G., Borthwick, P., Gorchkov, N., McGrattan, K., Forney, G., Grosshandler, W.L., Presser, C., and Melton, L., “Suppression of engine nacelle fires,” in Chapter 9, *Fire Suppression System Performance of Alternative Agents in Aircraft Engine and Dry Bay Laboratory Simulations*, Vol. II, Gann, R.G. (ed.), NIST SP 890, U.S. Department of Commerce, Washington, DC, November 1995.
- [8] DeMore, W.B., Sander, S.P., Golden, D.M., Hampson, R.F., Kurylo, M.J., Howard, C.J., Ravishankara, A.R., Kolb, C.E., and Molina M.J., “Chemical Kinetics and Photochemical Data for Use in Stratospheric Modeling, Evaluation: Number 12,” JPL Publication 97-4, January 15, 1997, Jet Propulsion Laboratory, California Institute of Technology, Pasadena, California.
- [9] Yang, J.C., Cleary, T.G., Huber, M.L., and Grosshandler, W.L., “Vapor Nucleation in a Cryogenic Fluid/Dissolved Nitrogen Mixture during Rapid Depressurization,” *Proc. Roy. Soc. London* **A455**: 1717-1738 (1999).
- [10] Yang, J.C., Huber, M.L., Vázquez, I., Boyer, C.I., and Weber, L., “Measured and Predicted Thermodynamics Properties of Selected Halon Alternative/Nitrogen Mixtures,” *International Journal of Refrigeration*, **20** (2): 96-105 (1997).